Technical report

Chapter 3 of *Intelligent Infrastructures*:

Prevention of emergency voltage collapses in electric power networks using hybrid predictive control

S. Leirens, R.R. Negenborn

If you want to cite this report, please use the following reference instead:

S. Leirens and R.R. Negenborn, "Prevention of emergency voltage collapses in electric power networks using hybrid predictive control," Chapter 3 in *Intelligent Infrastructures* (R.R. Negenborn, Z. Lukszo, and H. Hellendoorn, eds.), Dordrecht, The Netherlands: Springer, ISBN 978-90-481-3597-4, pp. 55–88, 2010.

Delft University of Technology, Delft, The Netherlands

Chapter 3
Prevention of Emergency Voltage Collapses in Electric Power Networks using Hybrid Predictive Control

S. Leirens and R.R. Negenborn

Abstract The reliable operation of electricity transport and distribution networks plays a crucial role in modern societies. However, too often, when a fault occurs in electricity networks, such as a transmission line drop, loss of generation, or any other important failure, voltages start to decay, potentially leading to complete blackouts with dramatic consequences. Thus, techniques are required that improve the power grid operation in case of emergencies. In this chapter, to achieve this aim, an approach is presented that uses an adaptive predictive control scheme. Electric power transmission networks are hereby considered as large-scale interconnected dynamical systems. First, voltage instability issues are illustrated on a 9-bus benchmark system. Then, the details of the proposed approach are discussed: the power network modeling and the construction of a hybrid prediction model (i.e., including both continuous and discrete dynamics), and the formulation and the resolution of the adaptive predictive control problem. In simulation studies on the 9-bus benchmark system the performance of the proposed approach is illustrated in various emergency voltage control cases.

S. Leirens
Universidad de Los Andes, Departamento de Ingeniería Eléctrica y Electrónica, Bogotá, Colombia,
e-mail: sleirens@uniandes.edu.co

R.R. Negenborn
Delft University of Technology, Delft Center for Systems and Control, Delft, The Netherlands,
e-mail: r.r.negenborn@tudelft.nl

3.1 Introduction

The human and economic consequences of power outages have shown that the reliable operation of electricity transport and distribution networks plays a crucial role in modern societies, as illustrated by recent problems in the United States and Canada, Europe, and Latin America [52–54]. The safe operation of the electricity network has to be carried out both under regular operating conditions, and also when the system is operating close to its limits. A great part of current research efforts is devoted to explore new ways to improve the power grid operation in terms of efficiency, reliability, and robustness, while satisfying constraints on economy and environment.

This is necessary, since electric power networks are experiencing rapid and important changes, in particular in the way they are operated and managed:

- The environmental opposition against the expansion of the physical power transportation infrastructure is now stronger than before, and the consumption of electricity increases in areas that are already heavily loaded [16];
- The development of interconnections between countries (e.g., in Europe) leads to very complex large-scale dynamical systems [24];
- New economic regulations due to the growth of energy markets induce unpredicted power flows and demand for a relaxation of security margins [10].
- The number of actors in the network increases as the amount of distributed or embedded generation increases, e.g., as industrial suppliers and households start to feed electricity into the network [20].

Due to the increased complexity arising from these aspects, the consequences of failures, such as transmission line drops, losses of generation, or any other important failures in the system, become more significant. The conventional control schemes of the network operators have to be revised, renewed, or even replaced by control schemes that can manage the electric power network of the future.

3.1.1 Power systems issues

In general, a power system is a strongly nonlinear system that have to be controlled over a wide range of operating conditions, possibly far from equilibrium points, in particular in emergency situations such as voltage instability [55]. The behavior of power systems is characterized by so-called hybrid behavior [2], i.e., behavior resulting from the interaction between continuous and discrete dynamics. Continuous dynamics of power systems are mainly driven by components such as generators and loads, and are usually represented by systems of differential-algebraic equations (DAEs). The discrete behavior arises from the nature of connected elements, such as capacitor banks, line breakers, and limiters in voltage regulators, or the way in which such elements are controlled, e.g., via discrete shedding of load, *on* or *off* switching of generation units, and on-load tap changing of ratio control in transformers. Moreover, power networks typically span a wide range of time scales and

large geographical areas. As a consequence, electric power networks are modeled as large-scale nonlinear hybrid systems.

Such complex systems are generally controlled in a hierarchical way and control takes place at different layers with a decomposition based on space and time divisions [5]. At the lowest layer, the controllers act directly on the actuators of the physical system with fast and localized control, e.g., single-input single-output controlled systems, such as automatic voltage regulators of synchronous machines. At the higher layers, supervisory controllers determine set-points for lower control layers in order to obtain coordination. Model-based approaches and global control for power systems become conceivable at these layers, since wide-area and phasor measurements are available [51], and utilities increasingly demand wide-area control, protection, and optimization systems [22].

Emergency voltage control deals with the problem of voltage instability leading to so-called *collapses* after disturbances [49, 50, 55]. The current protection schemes against voltage collapses are generally rule-based and consist of load shedding and reactive power compensation associated with strong operator training. However, the nonlinear behavior of power systems makes these rules strongly dependent on the operating conditions. After a disturbance such as breaking of a transmission line, the generation and transmission system may not have sufficient capacity to provide the loads with power. Voltage instability may then occur, in the worst case leading to total network blackouts. Voltage collapses are not only associated with weak systems such as power networks with low transfer capability, but are also a source of concern in highly developed networks that are heavily loaded. An illustration of this phenomenon is presented in Section 3.2.

The principal objective of the control system of an electricity network is to minimize the effects of the possible disturbances on the quality of the supplied energy [55], i.e.,

- voltages must remain within an acceptable range, e.g., within 5–10 % of the nominal value;
- requirements on physical limitations of interconnected elements must be satisfied,

while minimizing power losses, and achieving economic objectives, e.g., by minimizing the use of load shedding, since customers are then disconnected from the system, suffering great economical losses.

In the current power network operation, emergency voltage control is typically performed by human operators that are *in the loop*. The operators monitor the grid (typically power flows, voltage magnitudes, and angles) and take decisions following pre-established procedures. Decisions, such as on the *on* or *off* switching of equipment and the provision of set-points to lower control layers are based on offline studies, extensive experience, system conditions observed via telemetry, heuristics, knowledge bases, and state-estimator outputs. The control problem is then inherently complex and in general there is no possibility to rapidly change the operating conditions in an online and coordinated manner since the grid operation relies

mainly on the operators (*dispatchers*). New online control systems become increasingly necessary to face the recent changes in electricity networks and to achieve improved performance.

3.1.2 Power network modeling and control

Power networks are large-scale interconnected dynamical systems and their physical modeling relies on analytic models of individual components and knowledge of the network structure. General models at component level can be expressed in terms of the nonlinear dynamics of the local states, and input and output variables. These input and output variables are subject to algebraic constraints defined by Kirchhoff's laws. Hence, the combination of the dynamic models of the individual components and these algebraic constraints takes the form of a system of nonlinear DAEs [19].

Electric power systems consist of two types of fundamental components: single-port equipment components and two-port transmission components. Single-port equipment components are components such as synchronous machines and loads, including their primary controllers (governors, exciters, switched-shunt capacitors, and reactors). Two-port transmission components are components such as high-voltage transmission lines that connect buses (nodes in the network) and their primary controllers (series capacitors, phase-shifting transformers, and on-load tap changers) [19]. Single-port components are connected to other single-port components via two-port components. Each of these components is hereby described by its constitutive relations, the complexity degree of which can be very high. E.g., obtaining dynamic models of synchronous machines is an extremely laborious process [19, 25]. The equations of the component models can be nonlinear, hybrid, differential, and non-smooth. Simplifications are generally made with respect to the phenomena of interest, e.g., in the case of quasi-static models for voltage stability studies, for which fast dynamics, such as electromechanical dynamics, are neglected and frequency is assumed to be constant [55].

Despite the fact that models consisting of systems of DAEs attract much interest, due to their importance as models for a large class of dynamical processes (e.g., in mechanics, robotics, and chemical engineering), such models present intrinsic numerical difficulties. Systems of DAEs are more difficult to solve than systems of ordinary differential equations because of issues related to their index [17] and the determination of consistent initial conditions [8, 45].

To deal with control and optimization of systems modeled by DAEs, several strategies have been proposed, such as simultaneous strategies [6, 9, 21], multiple shooting strategies [11, 12], and direct search methods [43]. The particular structure of power network models (see Section 3.3.4) can especially be used advantageously to set up tractable models for model-based control approaches, such as model predictive control (MPC) [31]. MPC is a control methodology that has been successfully applied to a wide range of control problems, including problems in industrial processes [40], steam networks [32], residential energy resources [42], greenhouse systems [47], drug delivery systems [7], and water systems [44].

In MPC, a control action is obtained at discrete control sample steps by solving an optimization problem that minimizes an objective function over a finite receding horizon subject to the equations of a prediction model and operational constraints. The main advantages of MPC are:

- the explicit way of integrating present and future soft as well as hard constraints, such as operational constraints on bus voltages, line currents, generator excitations, and bounded control inputs and states, such as transformer ratios and reactive compensation units;
- the ease of integrating forecasts to anticipate events in the infrastructure, in the case that an event is known in advance to occur, such as an overloaded line disconnection, loss of generation, consumption changes, and maintenance actions;
- the ability to update online the prediction model to manage fast changing conditions in an adaptive way;
- the straightforward design procedure (see Section 3.4).

Given a model of the system to be controlled, hard constraints can be incorporated directly as inequalities and soft constraints can also be accounted for in the objective function by using penalties for violations. Fundamental trade-offs between efficiency and priorities are handled through the minimization of a cost function to fulfill economic objectives and minimize power losses.

As stated above, power systems belong to the class of hybrid systems. Conventional methods, i.e., either purely continuous or purely discrete methods, cannot be used for control of systems with both continuous and discrete dynamics. The control approach that is presented in this chapter is called a hybrid approach in the sense that it deal with both continuous and discrete dynamics at the same time in an integrated way.

MPC has first been applied to a voltage control problem in [26], in which a coordinated system protection scheme against voltage collapse using search and predictive control is presented. To be tractable, this approach uses a single-step linearized prediction model, that is, a constant control input is assumed over the entire prediction interval. This approach cannot handle discrete behavior. It is a small signal approach, in which all control variables are discretized leading to a purely combinatorial optimization problem.

In [18], the mixed-logical dynamical framework [4] is used to model the hybrid behavior of a 4-bus power system. In this approach the continuous state-input space is divided into several polytopes; a different affine model may be used for each combination of the values of the discrete variables. The gridding of the continuous state-input space has to be tight enough for good accuracy and leads to a great number of affine models. A trade-off has to be made between combinatorial complexity and required accuracy of the model. Using mixed-logical dynamical prediction models for MPC results in solving at each control step a mixed-integer programming problem [27, 30, 37].

The approach that is presented below is based on an adaptive hybrid MPC scheme. The power network equations are symbolically linearized and the hybrid

prediction model is updated online at the current operating point. Since the controller implements a model that is adapted to the operating point, the MPC-based hybrid strategy involves a reduced combinatorial complexity to the one induced by the discrete variables only, without partitioning the state-input space. A simple and suitable mixed optimization algorithm is proposed to solve the hybrid predictive control problem.

3.1.3 Outline

In Section 3.2 an illustration of the voltage instability phenomenon is presented using a 9-bus benchmark system, and current operating schemes are discussed. Section 3.3 presents the steps to build an accurate prediction model which captures the dynamics involved in voltage instability issues. The basic concepts of predictive control and the special features of the hybrid approach that is presented here as well as the solution of the hybrid MPC problem are presented in Section 3.4. In Section 3.5, the results of this approach applied to the 9-bus benchmark system are presented. Section 3.6 gives concluding remarks and directions for future research.

3.2 Power network operation

This section starts with illustrating voltage instability of power networks using a voltage collapse in a 9-bus benchmark system. This example shows that despite a set of corrective actions, the voltages collapse, mainly due to lack of coordination in the operation of the network. Then, operating schemes that could stabilize the network are presented.

3.2.1 Emergency scenario

A major source of power outages is voltage instability. This dynamic phenomenon arises when the individual controllers of the loads attempt to restore the consumed power beyond the capacity (physical limit) of the production-transport system [55]. This may occur following the outage of one or more components in the system, such that the load demand cannot be satisfied with a physically sustainable profile of the voltage plan, typically caused by voltage levels becoming very low. The reduced capacity of the network together with the requested load consumption requires coordinated corrective actions to avoid that involved dynamics drive the system into undesired or unacceptable states.

Consider the power system shown in Figure 3.1. This system represents a transmission network in which each generator is a simplified representation of an adjacent subnetwork. This benchmark system reproduces most of the phenomena of interest in power network dynamics, including in particular voltage instability and collapses. It is composed of the following elements and control devices:

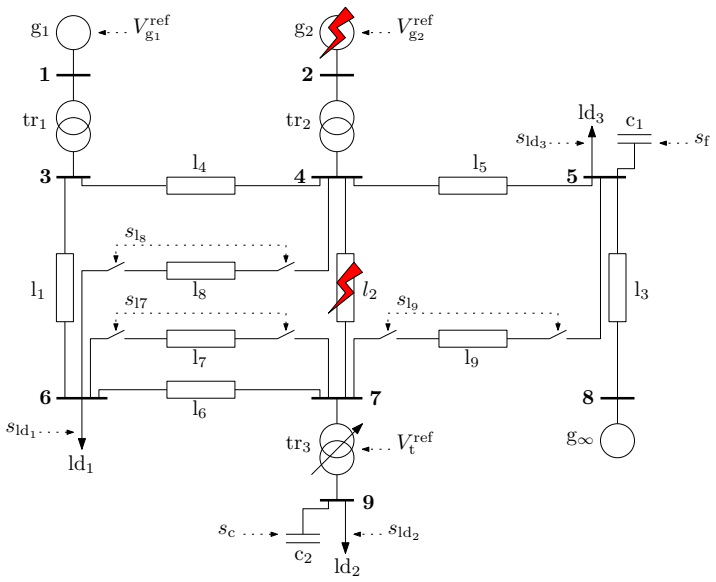

Figure 3.1: Overview of the 9-bus power network benchmark system.

- Generator g_∞ represents a large surrounding network and forces the voltage at bus 8 to stay constant.
- Generators g_1 and g_2 represent simplified models of adjacent subnetworks and are equipped with automatic voltage regulators and overexcitation limiters; they accept as control input the voltage references $V_{g_1}^{ref} \in [0.9, 1.1]$ and $V_{g_2}^{ref} \in [0.9, 1.1]$, respectively, for the automatic voltage regulators;
- Nine transmission lines, l_1–l_9, interconnect the components of the network. Three of them, l_7, l_8, and l_9, are equipped with controllable line breakers; these controllable lines have as control inputs s_{l_7}, s_{l_8}, and s_{l_9}, respectively, that can take on the values 1 (connected) or 0 (disconnected).
- A flexible AC transmission system c_1 is present for reactive power control; it is modeled as a continuously controlled capacitor with as control input the amount $s_f \in [0, 2]$ of reactive power injected into the network.
- A capacitor bank c_2 is present for additional reactive power compensation, using several separate units that can be connected or disconnected, with as control input the number $s_c \in \{0, 1, 2, 3\}$ of capacitor units connected to the network.
- The transformers tr_1 and tr_2 transform voltage magnitudes at fixed ratios.
- The transformer tr_3 is a transformer equipped with an on-load tap changer, which has as control input the voltage reference $V_t^{ref} \in [0.8, 1.2]$.
- The loads ld_1, ld_2, and ld_3 are dynamic loads representing groups of consumers with a voltage dependent behavior, i.e., active and reactive power recovery [23]. The loads can be shed, i.e., disconnected, using the control inputs s_{ld1}, s_{ld2}, and s_{ld3}, respectively, that take on the value 0 (no power shedding) or 1 (5% power shedding).

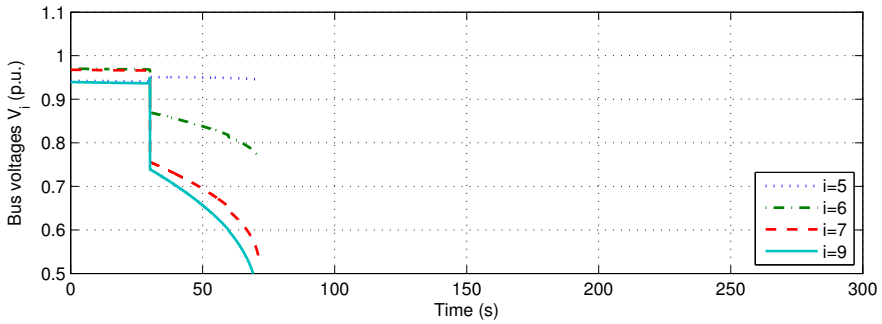

Figure 3.2: Voltage collapse after the loss of transmission line l_2.

The equations describing the elements of this network take on the form of a system of hybrid DAEs, in which the continuous dynamics arise from the loads (cf. Section 3.3.1.2), and discrete events occur when:

- a generator, g_1 or g_2, reaches the excitation limit (cf. Section 3.3.1);
- a line is connected or disconnected (l_7–l_9);
- a unit of capacitor banks c_2 is connected or disconnected;
- consumers are connected or disconnected from the grid (load shedding);
- the on-load tap changer of the transformer tr_3 changes the ratio tap by tap.

An event can be controllable or not. Line, capacitor and load switching events are controllable by inputs, whereas reaching the excitation limit or changing taps are uncontrollable events. A complete description of the parameters of the different models and numerical values can be found in [28].

Now consider a fault in line l_2 at $t = 30$ s. The breakers at both sides of the transmission line open and cause the transmission line to be disconnected. Figure 3.2 shows the evolution of the voltages when no control is employed. As can be seen, directly after the fault, voltages start to drop. Nothing is done to correct the evolution and the bus voltages collapse quickly.

3.2.2 Stabilizing operation

The purpose of emergency voltage control is to supply a set of corrective actions to apply to the system following an outage while fulfilling physical and operational constraints. Usually, the control objectives are specified as follows:

- to achieve a steady-state point of operation allowing the voltage plane to stay between 0.9 and 1.1 p.u, that is close to the nominal values, to fulfill requirements of safety and quality of energy;
- to optimize the use of control means to fulfill economic objectives, i.e., the use of reactive power compensation has to be preferred to load shedding, which is the ultimate control action since it disconnects consumers from the grid.

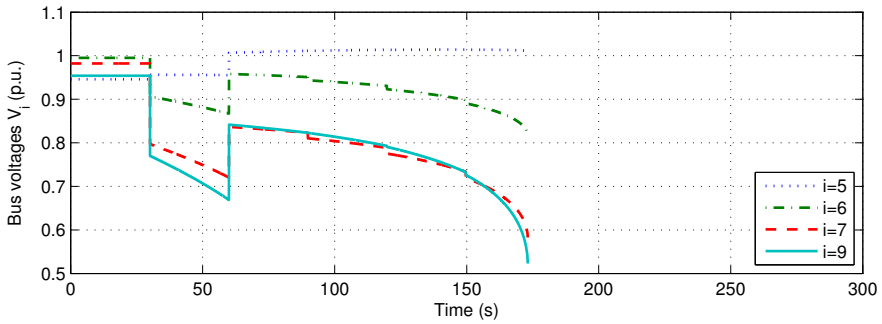

Figure 3.3: Voltage collapse under manual control after the loss of transmission line l_2.

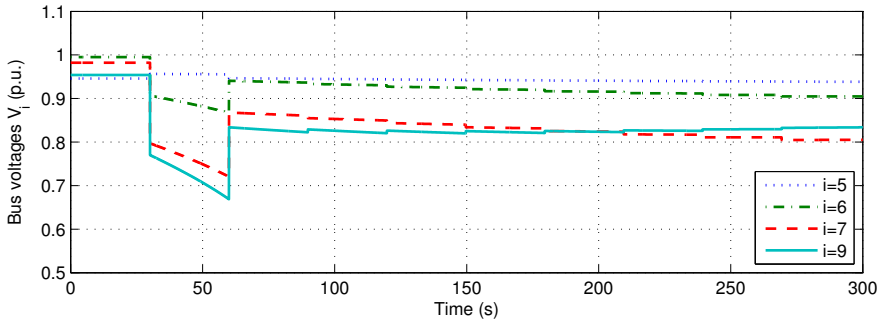

Figure 3.4: Stabilization of voltages after the loss of transmission line l_2.

The effects of corrective actions are illustrated with various cases. Consider the same fault as before, i.e., on line l_2. The breakers at both sides of the transmission line l_2 open at $t = 30$ s. At time $t = 60$ s, which is only 30 s after the disturbance, load shedding of 10% of all the consumption and maximum reactive power compensation (FACTS c_1 and capacitor bank c_2) are employed via *manual control*. As shown in Figure 3.3, this manual control is not sufficient to prevent a voltage collapse. The bus voltages start to collapse at the moment that the power consumption reaches the maximum transfer capability of the system (at $t \approx 100$ s).

Figures 3.4 and 3.5 illustrate the stabilization of the network dynamics in two different emergency situations. In Figure 3.4, 30 s after the loss of transmission line l_2, the topology of the network is modified with the connection of lines l_7 and l_8. The distribution of power flows is modified by the new configuration of the network and stability is recovered, but some buses have an unacceptably low voltage (V_7 is around 0.8 p.u.). Figure 3.5 shows the stabilization of the network dynamics after the loss of generator g_2. In this case, stability is recovered by using reactive power compensation (c_1 and c_2), modification of the reference voltage of the on-load tap changer of tr_3 and load shedding (ld_2 and ld_3).

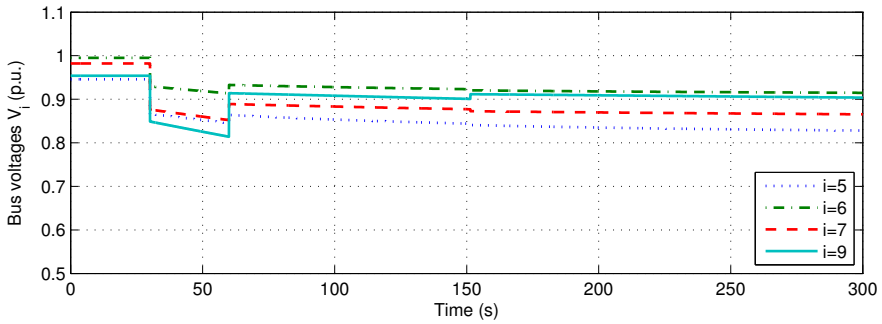

Figure 3.5: Stabilization of voltages after the loss of generator g_2.

In Section 3.3 and 3.4, an MPC-based method is proposed to determine the optimal corrective autonomously and automatically.

3.3 Hybrid dynamical models of power networks

The need for more accurate operation techniques as well as the available computation capabilities of modern computers call for new control methods and algorithms. The dynamics of the network hereby have to be taken into account as well as possible. This section presents the nonlinear and hybrid modeling aspects of electric power networks in the context of emergency voltage control.

3.3.1 Generation and consumption

The dynamics involved in voltage stability issues are said to be slow (the time constants are about 30–60 s) compared with electromechanical dynamics involved in frequency issues (transients lasting for a few seconds). Therefore, quasi-static or quasi-steady state models are commonly used in voltage stability studies [55]. In quasi-steady state models it is assumed that the frequency of the power network is constant, that is, fast dynamics are neglected and replaced with equilibrium equations. The in practice present three phases are assumed to be balanced reducing the models to equivalent one-line diagrams. Since the frequency is assumed to be constant, voltage, current, and state variables can be represented by so-called *phasors* [25], i.e., complex numbers that represent sinusoids.

In the remaining of this chapter, the following notations are used:

- Phasors are shown as capital letters with an overline, e.g., $\bar{V} = v_x + jv_y, \bar{I} = i_x + ji_y$.
- The magnitude of a phasor is shown by the capital letter of that phasor without the overline, e.g., $V = \sqrt{v_x^2 + v_y^2}$, $I = \sqrt{i_x^2 + i_y^2}$.
- Lowercase bold letters, e.g., $\mathbf{x}, \mathbf{y}$, correspond to column vectors. Superscript T denotes transpose. Therefore row vectors are denoted by $\mathbf{x}^T, \mathbf{y}^T$.

- A collection of phasors in a column vector is represented by a capital bold letter with an overline, e.g., $\bar{\mathbf{I}}$.
- Matrices are denoted by bold capital letters, e.g., $\mathbf{A}$.
- Time derivatives of variables are indicated with a dot, e.g., $\dot{x}$.

3.3.1.1 Generators

Generators are modeled using synchronous machine equations [25, 55]. Almost all variables and parameters are expressed in the per unit (p.u.) system [25], that is with respect to base quantities, i.e., the per unit system used for the stator is based on the three-phase nominal power and the voltage values of the machine.

In the following, indices d and q refer to direct and quadrature machine axis, respectively, and arrise from the Park transformation [25]. This transformation consists of replacing the three armature windings in a generator by three fictitious windings labelled d, q, and o, where the d and the q axis rotate together with the machine rotor. In balanced conditions, the o winding does not play any role and therefore it will not be considered here. Notice that also magnetic saturation is neglected.

Under the above mentioned assumptions, the generator is described by the differential equations [25, 55]:

$$\dot{\delta} = \omega - \omega_0 \tag{3.1}$$

$$\dot{\omega} = -\frac{D}{2H}\omega + \frac{\omega_0}{2H}\left(P_\mathrm{m} - P_\mathrm{g}\right) \tag{3.2}$$

$$\dot{E}'_q = \frac{-E'_q + E_\mathrm{f} - \left(X_d - X'_d\right)\left(i_{x\mathrm{g}}\sin\delta - i_{y\mathrm{g}}\cos\delta\right)}{T'_{d\mathrm{o}}}, \tag{3.3}$$

where for this generator, δ is the rotor angle (in rad), ω is the angular frequency (in rad/s), E'_q is the electromotive force (emf) behind the transient reactance (in p.u.), ω_0 is the nominal angular frequency (in rad/s), D is the damping coefficient (in p.u.), H is the inertia constant (in s), P_m is mechanical power (in p.u.) provided to the generator, and P_g is the active power produced by the generator (in p.u.), E_f is the exciter (or field) voltage (in p.u.), X_d is the direct-axis synchronous reactance (in p.u.), X'_d is the direct-axis transient reactance (in p.u.), $\bar{I}_\mathrm{g} = i_{x\mathrm{g}} + j i_{y\mathrm{g}}$ is the armature current phasor (in p.u.), and $T'_{d\mathrm{o}}$ is the open-circuit transient time constant (in p.u.).

The active power produced by the generator is given by:

$$P_\mathrm{g} = v_{x\mathrm{g}} i_{x\mathrm{g}} + v_{y\mathrm{g}} i_{y\mathrm{g}}, \tag{3.4}$$

where $\bar{V}_\mathrm{g} = v_{x\mathrm{g}} + j v_{y\mathrm{g}}$ is the armature voltage phasor (in p.u.), and where the real and imaginary parts of the armature current are:

$$i_{x\mathrm{g}} = \frac{\sin 2\delta}{2}\left(\frac{1}{X_q} - \frac{1}{X'_d}\right)\left(v_{x\mathrm{g}} - E'_q\cos\delta\right)$$

$$-\left(\frac{\cos^2\delta}{X_q}+\frac{\sin^2\delta}{X'_d}\right)\left(v_{yg}-E'_q\sin\delta\right) \tag{3.5}$$

$$i_{yg}=\left(\frac{\sin^2\delta}{X_q}+\frac{\cos^2\delta}{X'_d}\right)\left(v_{xg}-E'_q\cos\delta\right) +\frac{\sin 2\delta}{2}\left(\frac{1}{X'_d}-\frac{1}{X_q}\right)\left(v_{yg}-E'_q\sin\delta\right), \tag{3.6}$$

where X_q is the quadrature-axis synchronous reactance (in p.u.). The automatic voltage regulator that is considered is a proportional controller and the overexcitation limiter is modeled as a saturation element:

$$E_{\mathrm{f}}=\min\left(G\left(V_{\mathrm{g}}^{\mathrm{ref}}-V_{\mathrm{g}}\right),E_{\mathrm{f}}^{\mathrm{lim}}\right), \tag{3.7}$$

where G is the steady-state open-loop gain of the automatic voltage regulator (in p.u./p.u.), $V_{\mathrm{g}}^{\mathrm{ref}}$ is the reference voltage of the automatic voltage regulator (in p.u.), and $E_{\mathrm{f}}^{\mathrm{lim}}$ is the excitation limit of the overexcitation limiter (in p.u.).

The work presented in this chapter focuses on load dynamics since they are the *driving force* of voltage instability. Therefore a steady-state approximation of the generator equations (3.1)–(3.3) is used together with the algebraic equations (3.4)–(3.7).

Then the set of generator models of the network is grouped into the following nonlinear algebraic equation:

$$\mathbf{h}(\bar{\mathbf{V}}_{\mathrm{g}},\bar{\mathbf{I}}_{\mathrm{g}},\mathbf{V}_{\mathrm{g}}^{\mathrm{ref}})=\mathbf{0}, \tag{3.8}$$

where $\bar{\mathbf{V}}_{\mathrm{g}}$ and $\bar{\mathbf{I}}_{\mathrm{g}}$ are vectors of the voltage and the injected current phasors at the buses that connect the generators to the grid, respectively, and $\mathbf{V}_{\mathrm{g}}^{\mathrm{ref}}$ is a vector with reference voltages for the automatic voltage regulators.

3.3.1.2 Loads

Load is a common term for aggregates of many different devices that are mainly voltage dependent. Load dynamics are considered from the point of view of power recovery, i.e., after a voltage drop, the internal control systems of the load attempt to recover the consumed power at its nominal level [23]. Load dynamics are described by a smooth nonlinear differential equation:

$$T_P\dot{x_P}+x_P=P_{\mathrm{s}}(V_{\mathrm{ld}})+P_{\mathrm{t}}(V_{\mathrm{ld}}) \tag{3.9}$$

$$P_{\mathrm{ld}}=(1-s_{\mathrm{ld}}\,\sigma)\,(x_P+P_{\mathrm{t}}(V_{\mathrm{ld}})), \tag{3.10}$$

where x_P is a continuous state variable, V_{ld} is the load voltage magnitude, $P_{\mathrm{s}}(V_{\mathrm{ld}})=P_0V_{\mathrm{ld}}^{\alpha_{\mathrm{s}}}$ and $P_{\mathrm{t}}(V_{\mathrm{ld}})=P_0V_{\mathrm{ld}}^{\alpha_{\mathrm{t}}}$ are the steady-state and transient voltage dependencies, respectively, P_{ld} is the active power which is consumed by the load and T_P is the active power recovery time constant. A similar model is used for the reactive load

power considering the following variables: x_Q, $Q_s(V_{ld}) = Q_0 V_{ld}^{\beta_s}$, $Q_t(V_{ld}) = Q_0 V_{ld}^{\beta_t}$, Q_{ld} and T_Q. Constant σ represents a constant load shedding step, and s_{ld} is a discrete control variable that takes its values in a bounded discrete set. The internal state of the load is defined as $\mathbf{x}_{ld} = \begin{bmatrix} x_P & x_Q \end{bmatrix}^T$. The set of load models of the network is grouped into the following nonlinear state-space equations:

$$\dot{\mathbf{x}} = \mathbf{f}(\mathbf{x}, \bar{\mathbf{V}}_{ld}) \tag{3.11}$$

$$\bar{\mathbf{I}}_{ld} = \mathbf{g}(\mathbf{x}, \bar{\mathbf{V}}_{ld}, \mathbf{s}_{ld}), \tag{3.12}$$

where $\mathbf{x}$ is the vector of internal states, $\bar{\mathbf{V}}_{ld}$ and $\bar{\mathbf{I}}_{ld}$ are the vectors of voltage and absorbed current phasors at the buses that connect the loads to the grid, respectively, and $\mathbf{s}_{ld}$ is the vector of load shedding inputs.

3.3.2 Transmission system

The transmission system interconnects the generators to the loads and is composed of transformers, compensation devices such as capacitor banks and FACTS, and transmission lines. The respective models are detailed below.

3.3.2.1 Transformers

Transformers are modeled using a complex impedance $\bar{Z}_t$ in series with an ideal transformer whose ratio is denoted by n_t. Variables $\bar{V}_{t1}$ and $\bar{V}_t$ refer to the primary and secondary voltage transformer phasor, respectively. Similar notations are used for the current phasors $\bar{I}_{t1}$ and $\bar{I}_t$. The transformer is described by linear equations with respect to voltage and current phasors:

$$\bar{V}_t = n_t V_{t1} - n_t^2 \bar{Z}_t \bar{I}_t \tag{3.13}$$

$$\bar{I}_{t1} = n_t \bar{I}_t. \tag{3.14}$$

The presence of an on-load tap changer allows the ratio n_t to vary tap by tap within bounds. The sequential behavior of the on-load tap changer can be described by a discrete-time dynamic model:

$$n_t(k+1) = n_t(k) - n_{step}\, \xi(\Delta V(k)), \tag{3.15}$$

where $n_t(k)$ is the bounded transformer ratio at time step k, $\Delta V(k) = V_t(k) - V_t^{ref}(k)$ is the error between the secondary voltage magnitude V_t, i.e., at the output of the transformer, and the bounded reference voltage V_t^{ref} of the on-load tap changer, and n_{step} is the ratio step corresponding to one tap change. A function ξ (being a simplification of the function used in [48]) is used to determine when a tap change is made as follows:

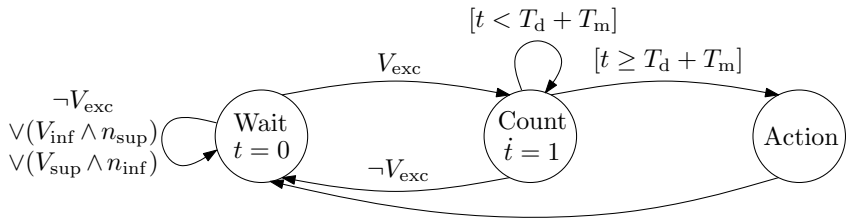

Figure 3.6: Finite-state machine for the on-load tap changer.

$$\xi(\Delta V) = \begin{cases} 1 & \text{if } \Delta V > \gamma \quad \text{for} \quad (T_\mathrm{d}+T_\mathrm{m})\,\mathrm{s} \\ -1 & \text{if } \Delta V < -\gamma \quad \text{for} \quad (T_\mathrm{d}+T_\mathrm{m})\,\mathrm{s} \\ 0 & \text{otherwise,} \end{cases} \tag{3.16}$$

where γ is the semi-deadband (or tolerance band) centered around $V_\mathrm{t}^\mathrm{ref}$, T_d is the time delay before a tap change is made, and T_m is the time necessary to perform the actual tap change. Depending on the type of on-load tap changer, T_d can be a constant or depend on ΔV. Since the size of a tap step is quite small (usually in the range of 0.5%–1.5% of the nominal ratio), to simplify the control design, n_t is considered as a bounded continuous variable.

The on-load tap changer used in the simulations presented in Section 3.5.2 is implemented using a finite state machine with three discrete states. Consider the logical variables (i.e., taking on values from the domain {true,false})

$$V_\mathrm{inf} \equiv \left[V_\mathrm{t} < V_\mathrm{t}^\mathrm{ref} - \gamma \right] \tag{3.17}$$

$$V_\mathrm{sup} \equiv \left[V_\mathrm{t} > V_\mathrm{t}^\mathrm{ref} + \gamma \right] \tag{3.18}$$

$$V_\mathrm{exc} \equiv V_\mathrm{inf} \vee V_\mathrm{sup} \tag{3.19}$$

and

$$n_\mathrm{inf} \equiv \left[n_\mathrm{t} \leq n_\mathrm{t}^\mathrm{min} \right] \tag{3.20}$$

$$n_\mathrm{sup} \equiv \left[n_\mathrm{t} \geq n_\mathrm{t}^\mathrm{max} \right], \tag{3.21}$$

where the symbol $\vee$ denotes the logical operator OR. The finite-state machine representing the tap changer is shown in Figure 3.6, where t refers to the internal timer variable and symbols $\neg$ and $\wedge$ refer to logical operators NOT and AND respectively. As long as the output voltage of the transformer stays inside the limits defined by the deadband or as long as a tap change is not possible, the on-load tap changer stays in the state *Wait*. When the voltage exceeds the deadband limits, the on-load tap changer enters in the state *Count*. If the voltage returns inside of the deadband limits before the timer reaches $T_\mathrm{d}+T_\mathrm{m}$, the state returns to *Wait*. If the internal timer

reaches $T_d + T_m$, the state becomes *Action*, a tap change is performed, and the state returns to *Wait*. More details about on-load tap changer dynamics can be found in [48] and [28]. The integration of the on-load tap changer dynamics in the prediction model is addressed in Section 3.3.4.

3.3.2.2 Reactive power compensation devices

Two kinds of reactive power compensation devices are considered: capacitor banks and FACTSs. A Capacitor bank is described by the following linear equation with respect to voltage and current phasors:

$$\bar{I}_c = j p_c s_c \bar{V}_c, \tag{3.22}$$

where a capacitor unit (susceptance) is represented by p_c and the number of connected units s_c can only take its values in a bounded discrete set.

A FACTS is considered here as a continuously varying capacitor and is described by the following linear equation with respect to voltage and current phasors:

$$\bar{I}_f = j p_f s_f \bar{V}_f, \tag{3.23}$$

where the total susceptance p_f is adjusted by a variable s_f that takes its value in a bounded continuous set.

3.3.2.3 Transmission lines

A transmission line is modeled using a complex impedance $\bar{Z}_l$:

$$\Delta\bar{V}_l = s_l \bar{Z}_l \bar{I}_l, \tag{3.24}$$

where $\Delta\bar{V}_l$ is the voltage across the line, i.e., the difference between two bus voltages, and $\bar{I}_l$ is the current through the line. If a line can be connected or disconnected in order to modify the network topology, a boolean control variable s_l is used to represent the state of the line: connected (1) or disconnected (0).

3.3.2.4 Complete transmission system

The transformer, compensation devices, and transmission line equations are linear with respect to voltage and current phasors. The complete transmission system model therefore consists of a system of linear algebraic equations:

$$\bar{\mathbf{w}}_{out} = \mathbf{M}\bar{\mathbf{w}}_{in}, \tag{3.25}$$

where $\bar{\mathbf{w}}_{out}$ and $\bar{\mathbf{w}}_{in}$ are generator and load voltages and currents phasors $\bar{\mathbf{V}}_{g,ld}$ and $\bar{\mathbf{I}}_{g,ld}$, respectively. Notice that the elements of matrix $\mathbf{M}$ depend on the variables $\mathbf{n}_t$, $\mathbf{s}_c$, $\mathbf{s}_f$ and $\mathbf{s}_l$.

3.3.3 Interconnected network

The hybrid nature of power systems is particularly characterized by the presence of two kinds of control inputs: discrete inputs arising from loads (s_{ld}), capacitor banks (s_{c}) and transmission lines (s_{l}), and continuous inputs arising from transformers (n_{t}) and FACTS devices (s_f). In the sequel, the discrete control vector is denoted by $\mathbf{u}_d = [\mathbf{s}_{\mathrm{ld}}^{\mathrm{T}}\ \mathbf{s}_{\mathrm{c}}^{\mathrm{T}}\ \mathbf{s}_{\mathrm{l}}^{\mathrm{T}}]^{\mathrm{T}}$ and the continuous control vector is denoted by $\mathbf{u}_{\mathrm{c}} = [\mathbf{n}_{\mathrm{t}}^{\mathrm{T}}\ \mathbf{s}_{\mathrm{f}}^{\mathrm{T}}]^{\mathrm{T}}$.

Discrete disturbances, such as transmission line drop and generator loss, together with the state of the generators (maximum excitation limitation) and the discrete control inputs define the discrete operating mode i of the network. The general power network model, defined by (3.8), (3.11)–(3.12), and (3.25), takes the form of a system of nonlinear and hybrid DAEs in each mode i:

$$\dot{\mathbf{x}} = \varphi_i(\mathbf{x}, \mathbf{y}, \mathbf{u}_c) \tag{3.26}$$

$$\mathbf{0} = \psi_i(\mathbf{x}, \mathbf{y}, \mathbf{u}_c)\,, \tag{3.27}$$

where $\mathbf{x}$ is the load state vector and the output vector $\mathbf{y}$ typically includes bus voltage magnitudes. This model is useful for performing simulations, as will be illustrated in Section 3.5. Nevertheless, simulating such a model requires dedicated algorithms, such as DASSL for solving the system of hybrid DAEs [8, 45], and particular special attention to the way in which the interactions between continuous and discrete dynamics are dealt with [13, 15].

3.3.4 Symbolic off-equilibrium linearization

Power systems are strongly nonlinear and to predict the system evolution, a feasible approach is to use locally a linear or, more generally, affine model. To obtain an accurate prediction model, (3.26)–(3.27) are symbolically linearized with respect to the continuous variables, i.e., the load state vector $\mathbf{x}$ and the continuous control input vector $\mathbf{u}_{\mathrm{c}}$. Note that

- the operating point $(\mathbf{x}_0, \mathbf{u}_{\mathrm{c}0})$ is not necessarily an equilibrium point. This kind of linearization is said to be *off-equilibrium*;
- the operating point $(\mathbf{x}_0, \mathbf{u}_{\mathrm{c}0})$ and the discrete mode i are symbolic parameters of the linearized model.

The evolution of the network can be predicted with accuracy using the linearized model, since the model that is used to compute the prediction is adapted based on the current operating point. Moreover, this modeling framework allows to handle the hybrid aspects explicitly. In the sequel, the operating point is assumed to be available or estimated. In practice, the operating point data are not available directly. All the measurement data are computed by an estimator and research efforts are made to improve methods and algorithms to estimate the network state online [39].

For small-scale power system such symbolic linearization may work well. However, almost all power systems are large-scale systems. The symbolic computation

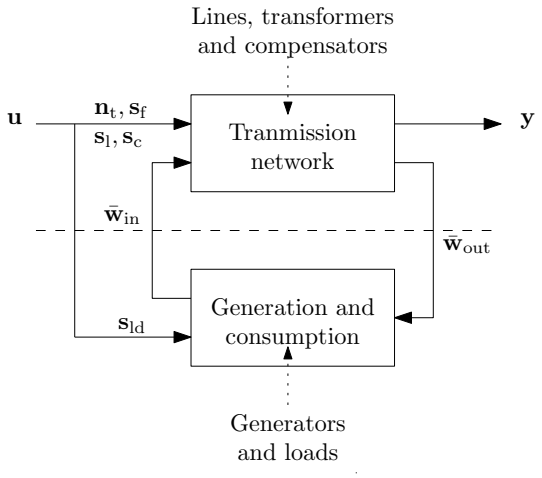

Figure 3.7: Decomposition of the power network into a linear and a nonlinear part.

required to directly linearize equations (3.26)–(3.27) becomes more and more complex with increasing network size. This complexity can be reduced by exploiting the particular structure of the equations. The generation and consumption part of the network (i.e., the generators and the loads) are modeled with a system of nonlinear equations, whereas the transmission part (i.e., the transmission lines, the compensation devices, and the transformers) are modeled with a system of linear equations. The model of the whole network can therefore be divided into two interconnected subsystems, as illustrated in Figure 3.7. The nonlinear subsystem is represented by (3.8) and (3.11)–(3.12). The linear subsystem is represented by (3.25). Note that by setting $\dot{\mathbf{x}} = 0$ in (3.11), a purely static problem that is similar to a load-flow calculation is obtained.

The linearized model is computed in two steps:

1. Equations (3.8) and (3.11)–(3.12) are symbolically linearized considering the symbolic parameters $\mathbf{x}_0$, $\mathbf{u}_{c0}$, and i. The computations are performed offline using the software package Mathematica [56] and lead to a set of Jacobian matrices parameterized by $\mathbf{x}_0$, $\mathbf{u}_{c0}$, and i.
2. The obtained symbolic model is updated online at each control step with the current values of the operating point $(\mathbf{x}_0, \mathbf{u}_{c0})$ and the discrete mode i. This update realizes the adaptation of the prediction model to the current operating conditions.

Time is discretized into discrete time steps $k = 0, 1, \ldots$, where discrete time step k corresponds to continuous time kT_s s, with T_s the sample period (s). Using the backward-Euler method to approximate the derivative, the following discrete-time affine model of the power network is obtained:

$$\mathbf{x}(k+1) = \mathbf{A}_i \mathbf{x}(k) + \mathbf{B}_i \mathbf{u}_c(k) + \mathbf{a}_i \tag{3.28}$$

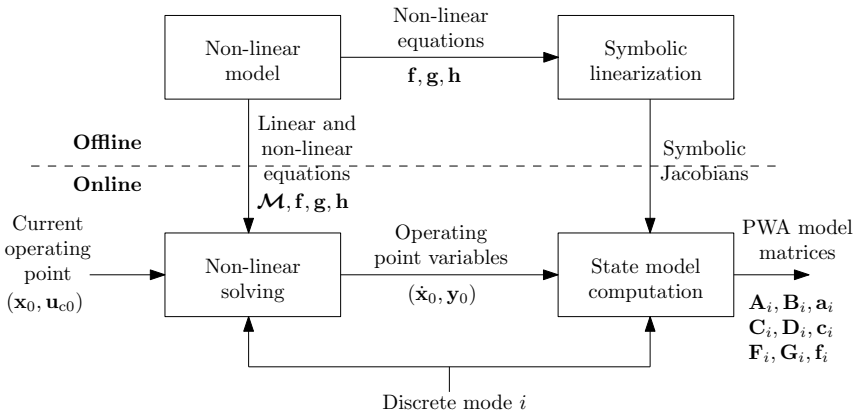

Figure 3.8: Overview of the computations of the predictions.

$$\mathbf{y}(k) = \mathbf{C}_i\mathbf{x}(k) + \mathbf{D}_i\mathbf{u}_c(k) + \mathbf{c}_i, \tag{3.29}$$

where the matrices $\mathbf{A}_i$, $\mathbf{B}_i$, $\mathbf{C}_i$, $\mathbf{D}_i$, and the vectors $\mathbf{a}_i$ and $\mathbf{c}_i$ depend on the discrete mode $i(k)$ and operating point $(\mathbf{x}_0(k), \mathbf{u}_{c0}(k))$, e.g., $\mathbf{A}_i = \mathbf{A}(\mathbf{x}_0(k), \mathbf{u}_{c0}(k), i(k))$. Furthermore, $\mathbf{u}_c(k)$ is the vector of continuous valued control inputs applied to the system from instant k to instant $k+1$, assumed to be constant over the sample period.

Due to the presence of generator excitation limiters, it is relevant to take into account the state of the generators in the prediction computation by adding to the model (3.28)–(3.29) the constraints:

$$\mathbf{F}_i\mathbf{x}(k) + \mathbf{G}_i\mathbf{u}_c(k) \leq \mathbf{f}_i. \tag{3.30}$$

These constraints in the continuous state-input space describe the state of the generators with respect to the discrete mode i. The resulting model has now a piecewise affine form and allows to predict the evolution of the state of the generators as well.

The linearization procedure is summarized in Figure 3.8. Note that the computational effort required by this approach is driven more by the number of connected generators and loads, than by the number of buses, since the computational effort depends strongly on the vector dimensions. The variables involved in these vectors are the voltage and current phasors that interconnect the generators and loads to the transmission system as defined in Section 3.3.2.

Special attention must be paid to the integration of the dynamics of on-load tap changers in the model. A good prediction requires that tap changes are synchronized with the control time steps, i.e., executed at the same time as control actions. A basic approach is to choose a sample time equal to the tap change delay and to introduce the following equation in the model (3.28)–(3.29):

$$n_t(k+1) = n_t(k) + \Delta n_t(k), \tag{3.31}$$

where n_t is now a state variable and the tap change Δn_t is a discrete control input with $\Delta n_\mathrm{t} \in \{-n_\mathrm{step}, 0, n_\mathrm{step}\}$. To control the on-load tap changer, a bang-bang control strategy is implemented locally:

$$V_\mathrm{t}^\mathrm{ref}(t) = \begin{cases} V_\mathrm{t}^\mathrm{ref,min} & \text{if} \quad \Delta n_\mathrm{t} = -n_\mathrm{step} \,, \\ V_\mathrm{t}^\mathrm{ref,max} & \text{if} \quad \Delta n_\mathrm{t} = n_\mathrm{step} \,, \\ V_\mathrm{t}(t) & \text{if} \quad \Delta n_\mathrm{t} = 0 \,, \end{cases} \tag{3.32}$$

where $V_\mathrm{t}^\mathrm{ref}$ is the on-load tap changer reference voltage, V_t is the secondary voltage of the transformer, $V_t^\mathrm{ref,min}$ and $V_t^\mathrm{ref,max}$ are the lower and upper bounds on $V_\mathrm{t}^\mathrm{ref}$, respectively, and n_step corresponds to one tap change of the transformer. The transformer ratio n_t between times k and $k+1$ is then consistent with the optimal value of Δn_t computed by the controller at time k. An extension to the case in which the sample time and tap change delay differ is proposed in [28].

A controller designed for the resulting piece-wise affine model is expected to control the behavior of the hybrid nonlinear system efficiently. At each time step, the model update requires a few computations and the controller only acts in a region close the operating point at which the system was linearized. In the next section a predictive control strategy for controlling power systems using the discussed modeling framework is presented.

3.4 Model predictive control

Model predictive control is based on solving online a finite time optimal control problem using a receding horizon approach, as summarized in the following steps [31]:

- At time step k and for the current state $\mathbf{x}(k)$, an open-loop optimal control problem over a future time interval is solved online, taking into account the current and future constraints on input, output, and state variables. This results in a sequence of actions over that future time interval that gives the best predicted performance.
- The first action in the optimal control sequence so obtained is applied to the system.
- The procedure is repeated at time $k+1$ using the newly obtained state $\mathbf{x}(k+1)$.

The solution is converted into a closed-loop strategy by using the measured or estimated value of $\mathbf{x}(k)$ as the current state. The stability of the resulting feedback system can be established by using the fact that the cost function can act as a Lyapunov function for the closed-loop system [36].

3.4.1 Formulation of the control problem

Let $\mathbf{U}_N$ be the sequence of control inputs over the prediction horizon with a length of N time steps:

$$\mathbf{U}_N = [\mathbf{u}^{\mathrm{T}}(0)\ \mathbf{u}^{\mathrm{T}}(1)\ \cdots\ \mathbf{u}^{\mathrm{T}}(N-1)]^{\mathrm{T}}, \tag{3.33}$$

where $\mathbf{u}(k) = [\mathbf{u}_{\mathrm{c}}^{\mathrm{T}}(k)\ \mathbf{u}_{\mathrm{d}}^{\mathrm{T}}(k)]^{\mathrm{T}}$, and given the following cost function or performance index:

$$J_N(\mathbf{x}(0), \mathbf{U}_N) = F(\mathbf{x}(N)) + \sum_{k=0}^{N-1} L(\mathbf{x}(k), \mathbf{u}(k)). \tag{3.34}$$

In practice, the cost function to be optimized usually includes a term based on the state $\mathbf{x}(k)$ and a reference $\mathbf{x}_{\mathrm{r}}(k)$, and a term based on the control inputs $\mathbf{u}(k)$:

$$L(\mathbf{x}(k), \mathbf{u}(k)) = \|\mathbf{x}(k+1) - \mathbf{x}_{\mathrm{r}}(k)\|_{\mathbf{Q}_x} + \|\mathbf{u}(k)\|_{\mathbf{Q}_u}, \tag{3.35}$$

and a term based on the final state $\mathbf{x}(N)$:

$$F(\mathbf{x}(N)) = \|\mathbf{x}(N) - \mathbf{x}_{\mathrm{r}}(N)\|_{\mathbf{Q}_{\mathrm{f}}}, \tag{3.36}$$

where $\|\mathbf{w}\|_{\mathbf{Q}}$ denotes the 2-norm of a vector $\mathbf{w}$ with weighting matrix $\mathbf{Q}$. The weighting matrices are such that $\mathbf{Q}_x \geq 0$, $\mathbf{Q}_u > 0$ (by taking into account the constraints on $\mathbf{u}$, typically actuator constraints, it is sufficient for the matrix $\mathbf{Q}_u$ to be semi-positive definite) and $\mathbf{Q}_{\mathrm{f}} \geq 0$.

At each time step, the following optimization problem $\mathcal{P}_N$ has to be solved, where the superscript o here refers to optimality:

$$\mathcal{P}_N(\mathbf{x}(0))\ :\ J_N^{\mathrm{o}}(\mathbf{x}(0)) = \min_{\mathbf{U}_N} J_N(\mathbf{x}(0), \mathbf{U}_N), \tag{3.37}$$

while satisfying the power network model constraints (3.28)–(3.30) over the prediction horizon[1] Additional constraints may allow to include some knowledge about the system that is not captured by the model, such as actuator limitations and physical limits on state variables. On the one hand, input constraints take into account actuator limits over the prediction horizon and thus are considered as hard constraints. On the other hand, output limits are generally not considered as hard constraints, since the optimization problem $\mathcal{P}_N$ could then become infeasible. The constraints on the outputs are therefore usually softened by adding slack variables $\mathbf{s}$ that represent the amount of constraint violation, and that are constrained as

$$\mathbf{y}_{\mathrm{inf}} - \mathbf{s}(k) \leq \mathbf{y}(k) \leq \mathbf{y}_{\mathrm{sup}} + \mathbf{s}(k), \tag{3.38}$$

[1] Note that the PWA model is time invariant over the prediction horizon, but not over several time steps: at each time step the matrices have to be updated to the current operating point.

and for which the penalty term $\|\mathbf{s}(k)\|_{Q_s}$ is added to (3.35). Thus, an optimal solution of the MPC optimization problem (3.37) can be found while minimizing the constraint violations. A final state constraint $\mathbf{x}(N) = \mathbf{x}_f$ can be added to guarantee the stability of the closed-loop system [36], but attention has to be paid to the feasibility of the optimization problem (3.37).

An important characteristic of the optimization problem (3.37) is its mixed nature. The presence of both the continuous inputs ($\mathbf{u}_c$) and the discrete inputs ($\mathbf{u}_d$) causes having to find the control sequence $\mathbf{U}_N$ as the sequence of both the continuous inputs $\mathbf{U}_{cN}$ and the discrete inputs $\mathbf{U}_{dN}$ over the prediction horizon with length N. Hence:

$$J_N^o(\mathbf{x}(0)) = \min_{\mathbf{U}_{dN}} \left(\min_{\mathbf{U}_{cN}} J_N(\mathbf{x}(0), (\mathbf{U}_{cN}, \mathbf{U}_{dN})) \right), \tag{3.39}$$

subject to the model constraints, for $k = 0, 1, \cdots, N-1$:

$$\mathbf{x}(k+1) = \mathbf{A}_i\mathbf{x}(k) + \mathbf{B}_i\mathbf{u}_c(k) + \mathbf{a}_i \tag{3.40}$$

$$\mathbf{y}(k) = \mathbf{C}_i\mathbf{x}(k) + \mathbf{D}_i\mathbf{u}_c(k) + \mathbf{c}_i \tag{3.41}$$

$$\mathbf{F}_i\mathbf{x}(k) + \mathbf{G}_i\mathbf{u}_c(k) \leq \mathbf{f}_i, \tag{3.42}$$

where $i(k)$ is a function of $\mathbf{x}(k)$, $\mathbf{u}_c(k)$ and $\mathbf{u}_d(k)$.

Let $\mathbf{I}_N = \begin{bmatrix} i(0) & i(1) & \cdots & i(N-1) \end{bmatrix}^T \in \mathbb{I}$ be a sequence of modes over the horizon N, where $\mathbb{I}$ is the set of admissible sequences. A sequence $\mathbf{I}_N$ defines $\mathbf{U}_{dN}$ and N sets of constraints (3.40)–(3.42) for $k = 0, 1, \cdots N-1$. The problem $\mathcal{P}_N$ can now be reformulated as:

$$J_N^o(\mathbf{x}(0)) = \min_{\mathbf{I}_N} \left(\min_{\mathbf{U}_{cN}} J_N(\mathbf{x}(0), (\mathbf{U}_{cN}, \mathbf{I}_N)) \right). \tag{3.43}$$

Then, for a given sequence of modes $\mathbf{I}_N$, the cost

$$J_N^*(\mathbf{x}(0), \mathbf{I}_N) = \min_{\mathbf{U}_{cN}} J_N(\mathbf{x}(0), (\mathbf{U}_{cN}, \mathbf{I}_N)) \tag{3.44}$$

is the optimal cost that is found by solving a continuous constrained optimization subproblem. This subproblem can easily be reformulated as a standard quadratic programming (QP) problem. The superscript $*$ here refers to optimality with respect to a given sequence of modes $\mathbf{I}_N$. However, the constrained optimization subproblem (3.44) is not necessarily feasible, i.e., for a given sequence $\mathbf{I}_N$ it could be the case that no solution satisfies the model constraints (3.40)–(3.42) over the prediction horizon.

Due to the presence of the discrete variables, $\mathcal{P}_N$ is categorized as an NP-hard problem. In addition, since $\mathcal{P}_N$ also involves continuous variables, it is a so-called mixed-integer problem. A branch-and-bound algorithm will be used to solve the problem $\mathcal{P}_N$ efficiently. This algorithm basically consists of a best-first descent strategy to reach suboptimal solutions and a branch-cutting strategy to profit from

partial-horizon cost evaluation and infeasible subproblems. Below the details of this algorithm are discussed.

3.4.2 Mixed-integer optimization

The optimization problem associated with the predictive control of a piece-wise affine prediction model has been formulated above. This section is dedicated to the presentation of a simple, yet suitable mixed-integer optimization algorithm for hybrid MPC problems.

3.4.2.1 Exhaustive enumeration

The easiest way to find the optimal solution of the mixed-integer optimization problem consists of first enumerating all the possible sequences of modes over the prediction horizon and then solving the QP subproblems associated with each of these mode sequences. For a given sequence of modes, two situations with respect to a QP subproblem can occur: either the subproblem has no solution that satisfies the constraints (infeasibility), or the QP subproblem is feasible. For each feasible sequence $\mathbf{I}_N$ (defining a discrete control sequence $\mathbf{U}_{\mathrm{d}N}$) an optimal continuous control sequence $\mathbf{U}^*_{\mathrm{c}N}$ and a corresponding cost $J^*_N(\mathbf{x}(0), \mathbf{I}_N)$ can be obtained. The optimal solution is then given by the sequence of modes that minimizes (3.44):

$$J^{\mathrm{o}}_N(\mathbf{x}(k)) = \min_{\mathbf{I}_N} \left(J^*_N(\mathbf{x}(k), \mathbf{I}_N) \right). \tag{3.45}$$

This method, which is referred to as exhaustive enumeration, quickly becomes useless when the number of modes, or the length of the prediction horizon increases, since the control problem to be solved is NP hard. The number of possible mode sequences to enumerate over grows exponentially with the number of modes and the length of the prediction horizon. Let p be the number of possible modes of the system. The exhaustive enumeration of all mode sequences requires p^N QP subproblems to be solved.

Figure 3.9 depicts as a tree the various possibilities of mode sequences. The depth of the tree of possibilities grows with the length of the horizon. For a given depth, the width of the tree is fixed by the number of possible modes of the system. Each leaf is a QP subproblem to be solved and one of them yields the optimum searched for. The dimension of the decision vector of all the QP subproblems is identical, i.e., $\dim(\mathbf{U}_{\mathrm{c}}) = \dim(\mathbf{u}_{\mathrm{c}}) \times N$. All leaves of the tree for which the associated QP subproblem is feasible are suboptimal solutions, except for that feasible subproblem that yields the solution with the lowest cost of all. This is the optimal solution.

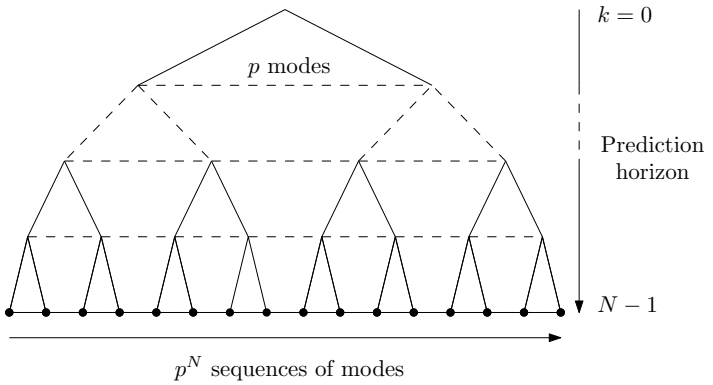

Figure 3.9: Illustration of exhaustive enumeration.

3.4.2.2 Partial enumeration

Exhaustive enumeration involves completely searching through the tree of possibilities. It is possible, however, to exploit the structure of the optimization problem associated with the hybrid predictive control scheme: the cost function of the optimization problem is additive, and has only positive terms. The key idea of the proposed partial enumeration algorithm is: given a suboptimal solution of (3.39)–(3.42), evaluate partial costs in order to prune the tree, i.e., cut branches that cannot lead to the optimum. This idea results in a branch-and-bound algorithm.

For a partial horizon P ($P < N$), i.e., at a depth P in the tree, the partial cost is defined as:

$$J_P(\mathbf{x}(0), \mathbf{U}_P) = \sum_{k=0}^{P-1} L(\mathbf{x}(k), \mathbf{u}(k)). \tag{3.46}$$

The proposed approach is a recursive algorithm that consists of a descent strategy and a branch-cutting criterion. The algorithm explores the tree according to the descent strategy, starting with a one step prediction horizon and increasing it step by step. The branch-cutting criterion allows to reduce the number of branches to consider and then to not explore the whole tree.

Descent strategy

Assume that the algorithm is at a depth P (with $P < N$) in the tree of possibilities, i.e., P time steps in the future. The proposed descent strategy is a *best-first* strategy:

- Compute the optimal costs J_{P+1} associated with the feasible subproblems for the possible choices of mode i.
- Choose the branch, i.e., the mode, that gives the minimal cost over the prediction horizon $P+1$ to continue the exploration.

Branch cutting

Assume that a first suboptimal solution is available, i.e., an upper bound on the optimal cost is available. Prune the tree by cutting the branches for which

- either the optimal cost on a partial horizon is greater than the cost of the suboptimum,
- or the subproblem is infeasible.

Cutting a particular branch means eliminating all branches originating from that particular branch. The best suboptimum so far is updated each time a leaf is evaluated and determined to have a cost that is lower than the cost of the previous best suboptimum.

3.4.2.3 Justification and illustration

Now some details are given to justify that the partial enumeration algorithm guarantees to find the optimum. Let a sequence of N modes $\mathbf{I}_N$ (the associated QP subproblem is assumed to be feasible) and a horizon P with $P < N$ be given. Below, the following notations are used:

- $\mathbf{I}_P^{(N)}$ is the sequence of the P first modes extracted from the sequence $\mathbf{I}_N$;
- $\mathbf{U}_{\mathrm{c}P}^{(N)}$ is the continuous control sequence of length P extracted from the sequence $\mathbf{U}_{\mathrm{c}N}$.

Recall that the superscript $*$ refers to optimality with respect to a given sequence of modes, i.e., the sequence $\mathbf{U}_{\mathrm{c}N}^{*}$ is optimal with respect to a given sequence of modes $\mathbf{I}_N$. However, the extracted sequence $\mathbf{U}_{\mathrm{c}P}^{*(N)}$ is not necessarily optimal over the partial horizon P.

Given a sequence of modes $\mathbf{I}_N$, for all $P < N$, the optimal cost that is obtained for the sequence $\mathbf{I}_N$ is greater than the optimal cost that is obtained for an extracted sequence $\mathbf{I}_P^{(N)}$:

$$\forall P < N,\ \ J_N^*\big(\mathbf{x}(0), \mathbf{I}_N\big) \geq J_P^*\big(\mathbf{x}(0), \mathbf{I}_P^{(N)}\big). \tag{3.47}$$

For a detailed proof of this statement, see [29].

Assume the algorithm to be arrived at a depth $P < N$ and that the associated cost J_P is greater than a prevously computed suboptimum. With respect to (3.47), the corresponding branch and all the following ones can be cut. An example of the execution of the proposed algorithm is illustrated in Figure 3.10.

The partial-enumeration algorithm is a branch-and-bound algorithm that leads to the optimal solution by taking advantage of the particular structure of the optimization problem associated with predictive control. General mixed-integer programming does not exploit this feature.

The proposed descent strategy is a heuristic that is likely to reach a first suboptimum close to the optimum. In fact, the suboptimal character comes from the choice of the sequence of modes (the best-first strategy at one prediction step), but the suboptimum is obtained by solving a QP subproblem over the full horizon with length N. In this partial enumeration approach, the dimension of the solution vector of the

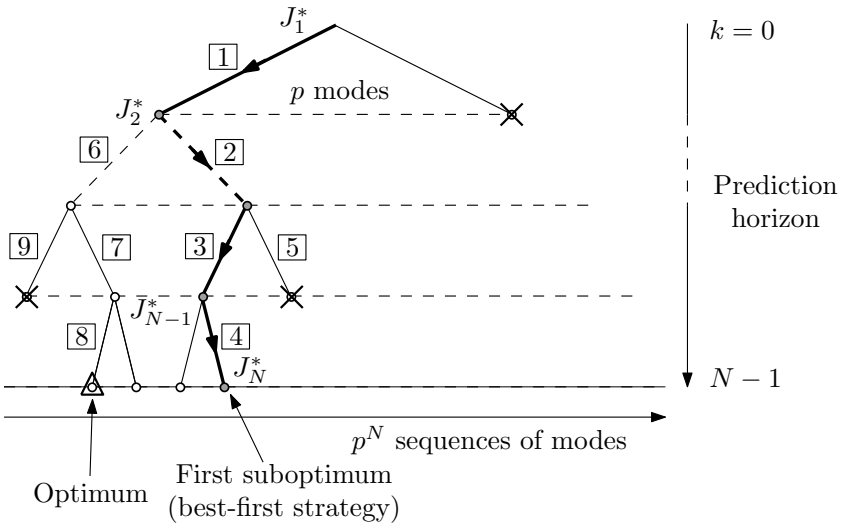

Figure 3.10: Illustration of execution of partial enumeration. *Numbers* indicate the route followed in the tree, i.e., the way in which the tree has been explored. *Bold lines* indicate the path to the first suboptimum (best-first strategy). The presence of a *cross* is the result of a branch cutting action: the cost were greater than the cost of the known suboptimum, or the subproblem was infeasible. The optimum search for is marked out by a *triangle*.

QP subproblems to be solved starts with $\dim(\mathbf{u}_c)$ at the top of the tree (one time step prediction) to grow with the horizon until reaching $\dim(\mathbf{u}_c) \times N$ at the bottom of the tree (using a horizon with length N).

3.5 Simulation studies

In this section, first the object-oriented concepts for modeling and simulation of the electricity network introduced in Section 3.2 are briefly presented. Then, simulation results of the proposed control approach are presented and discussed.

3.5.1 Simulation tools

To face the difficulty of developing complex power network models, object-oriented approaches for analysis and simulation of power systems have received increasing attention [33]. In object-oriented modeling, models are mapped as closely as possible to the corresponding physical subsystems that make up the overall system. Models are described in a declarative way, i.e., only local equations of the objects and the connections between the objects are defined. *Inheritance* and *composition* concepts enable proper structuring of models and generally lead to more flexible,

modular, and reusable models. Extended models can be constructed by inheriting dynamics and properties of more basic models.

As stated above the dynamics of power networks involve continuous and discrete dynamics and are therefore hybrid. Each of the objects of a power network can therefore be modeled with a mixture of differential equations, algebraic equations, and discrete-event logic, e.g., in the form of if-then-else rules. The model of the overall system then consists of the models for the objects and in addition algebraic equations interconnecting the individual objects.

Several object-oriented approaches have been developed over the years, e.g., [3, 13, 35, 38, 46]. These approaches typically support both high-level modeling by composition and detailed component modeling using equations. Models of system components are typically organized in model libraries. A component model may be a composite model to support hierarchical modeling and specify the system topology in terms of components and connections between them. Using a graphical model editor, e.g., Dymola [13], a model can be defined by drawing a composition diagram by positioning icons that represent the models of the components, drawing connections, and giving parameter values in dialog boxes.

Some of the object-oriented simulation software packages, such as Simulink, assume that a system can be decomposed into sub-models with fixed causal interactions [1]. This means that the models can be expressed as the interconnection of sub-models with an explicit state-space form. Often a significant effort in terms of analysis and analytical transformations is required to obtain a model in this form [13]. In general, causality is not assigned in power networks. Setting the causality of an element of the power network, e.g., a transmission line, involves representing the model equations in an explicit input-output form. In a voltage-current formulation this means that currents are expressed as function of voltages, or vice versa. Non-causal modeling permits to relax the causality constraint and allows to focus on the elements and the way these elements are connected to each other, i.e., the system's topology. For an example of the use of a non-causal and object-oriented approach for power system modeling, see [41].

An environment that allows non-causal modeling, and that was used in this work, is Dymola [13], which implements the object-oriented modeling language Modelica [38]. Figure 3.11 and 3.12 illustrate the implementation of the 9-bus benchmark system in the Dymola environment. The Dymola-Simulink Interface [14] allows to easily use a simulation model (implemented in Dymola) in the Matlab-Simulink environment.

3.5.2 Simulation results

The hybrid predictive control algorithm presented in Section 3.4 has been implemented in Matlab and applied to the 9-bus power network introduced in Section 3.2 (cf. Figure 3.1).

This benchmark system has a strong combinatorial nature since almost all the control variables take on discrete values. The major difficulty in the mixed opti-

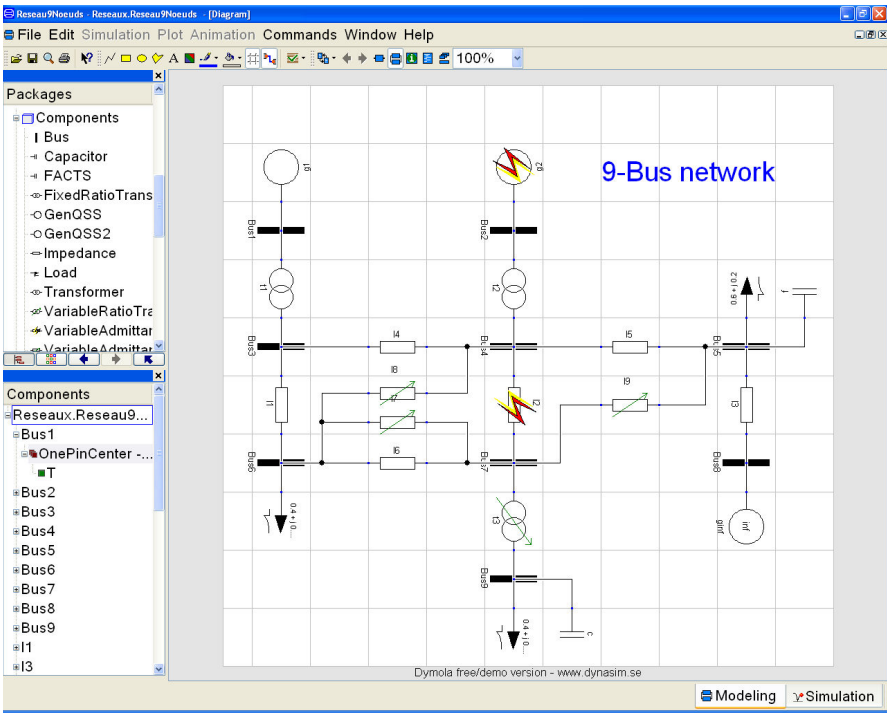

Figure 3.11: Illustration of the 9-bus network implemented in Dymola.

mization problem associated to the hybrid MPC formulation for this system is the number of discrete variables. Notice that an increase in the number of continuous variables does not significantly increase the complexity of the control problem.

To simulate the power system, a full nonlinear model has been implemented in Dymola [13] and simulations have been performed using the software package Matlab [34]. The sample period is $T_s = 30\,\text{s}$ and the prediction horizon is $N = 3$, such that the settling time of the load dynamics ($T_{P,Q} = 60\,\text{s}$) is exceeded. The controller has been tuned using weighting matrices according to the formulation presented in Section 3.4. The use of reactive power compensation devices and transformer ratio changes is slightly penalized. On the contrary, line reconfiguration and load shedding is more penalized, since the economic cost of these actions is much higher. Voltage deviations of the buses to which consumers (loads) are connected are penalized most. A full description of the numeric values of the tuning parameters can be found in [28].

Below the results of transmission-line drop and generator-loss contingencies are discussed.

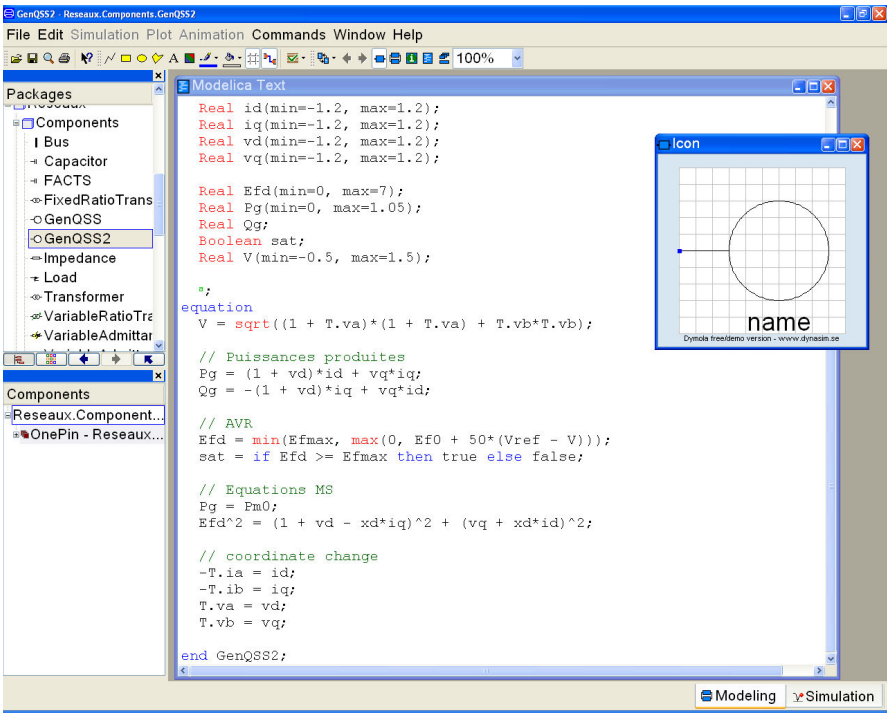

Figure 3.12: Illustration of the 9-bus network implemented in Dymola (equation side).

3.5.2.1 Scenario 1: Transmission line drop

In this scenario, transmission line l_2 is lost, i.e., unintentionally disconnected, at $t = 30$ s. Figures 3.13–3.14 show the results obtained when using the adaptive predictive control approach. In Figure 3.13, voltage stability is recovered 30 s after the fault has occurred, and all the voltages remain above 0.9 p.u. A new steady-state point of operation has been reached without using load shedding. Figure 3.14 shows the evolution of the control inputs over time. As can be observed, the solution determined by the controller mainly consists of injecting all the remaining reserve of reactive power (c_1 and c_2) and to connect transmission line l_9 at time $t = 60$ s. The controller acts in a coordinated manner on the other devices too, such as the generators and FACTS c_1 to keep the variables in acceptable ranges.

3.5.2.2 Scenario 2: Transmission line drop with parameter uncertainty

The same line drop scenario as above is considered, but now now the actual consumption of the loads at buses 5, 6 and 9 have been increased by 10%. The predictive controller is not aware of this, and, hence, uses values that not correct. In this way, the robustness of the controlled system to parametric uncertainty is illustrated.

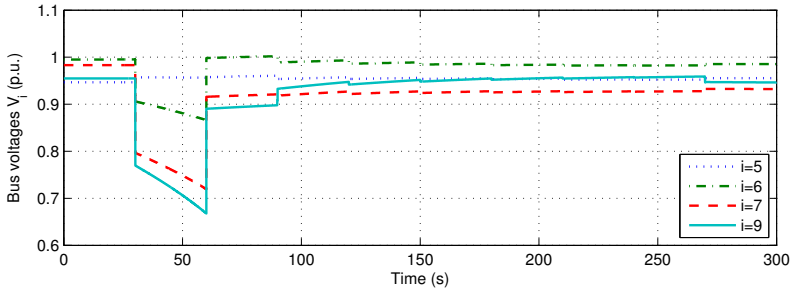

Figure 3.13: Bus voltage magnitudes (loss of transmission line l_2, nominal model).

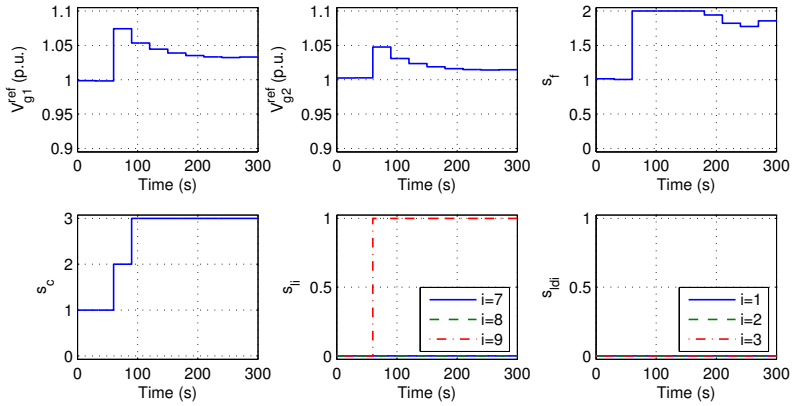

Figure 3.14: Control inputs (loss of transmission line l_2, nominal model).

Figures 3.15–3.16 indicate that for this scenario, the stability of the system is recovered, although the bus voltages cannot be maintained above 0.9 p.u. without using load shedding. If the actual load is more than 10% of the load assumed by the controller, the collapse is too fast for the controller to take adequate actions. In that case, the sample time T_s of the controller should be decreased if the systems has to stabilized.

3.5.2.3 Scenario 3: Generator loss

In this scenario, generator g_2 is lost, i.e., it is isolated from the grid. Figures 3.17–3.18 show the evolution of the network variables after the loss of the generator. To manage the loss of this generator, the controller uses load shedding of ld_2 and transmission line l_9 is connected at time $t = 60$ s. At the next time step, i.e., $t = 90$ s, the controller disconnects 5% of load ld_3. All the reactive compensation is used and the maximum excitation limit is reached for generator g_1. The network is stabilized at a new operating point, although some of the bus voltages are low, e.g., $V_5 < 0.9$ p.u.

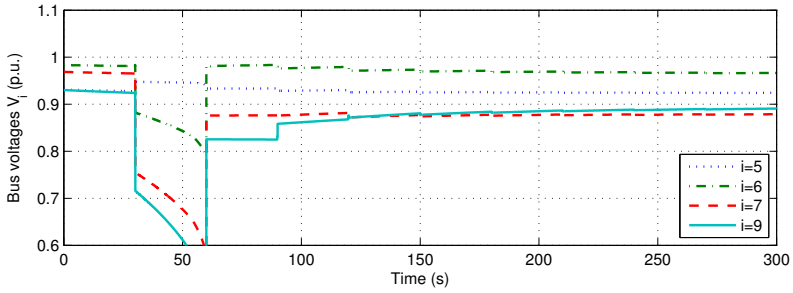

Figure 3.15: Bus voltage magnitudes (loss of transmission line l_2, 10 % consumption increase).

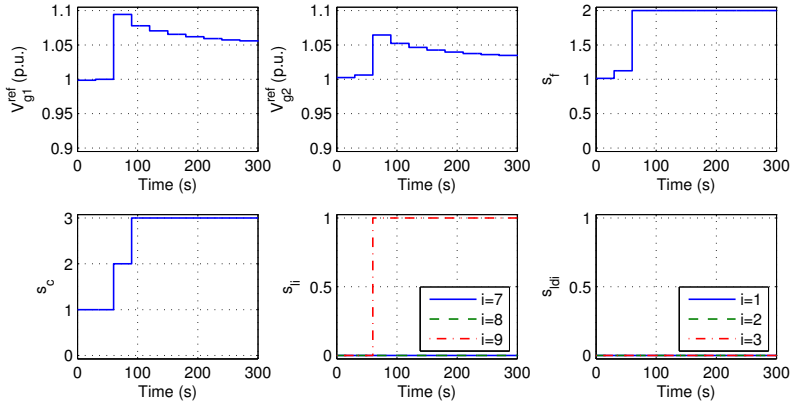

Figure 3.16: Control inputs (loss of transmission line l_2, 10 % consumption increase).

3.6 Conclusions and future research

This chapter has discussed the concepts of voltage stability of electric power networks and the possibly dramatic consequences of such instabilities, such as complete blackouts. Power networks are large-scale, nonlinear, and hybrid systems. An adaptive, model predictive control (MPC) approach for solving the emergency voltage control problem in such systems has been proposed. This approach uses a symbolically off-equilibrium linearized prediction model to deal efficiently with the hybrid and nonlinear characteristics of the dynamics involved. The symbolic linearization is based on a decomposition of the network into two interconnected subsystems and is performed offline to minimize the computational efforts required to update the hybrid prediction model at each time step online. Simulation studies on a 9-bus benchmark system have illustrated the performance of the proposed approach in line and generator loss case studies.

The proposed approach is not restricted to control of power networks alone. Also in other types of infrastructure systems, such as water networks and road traffic net-

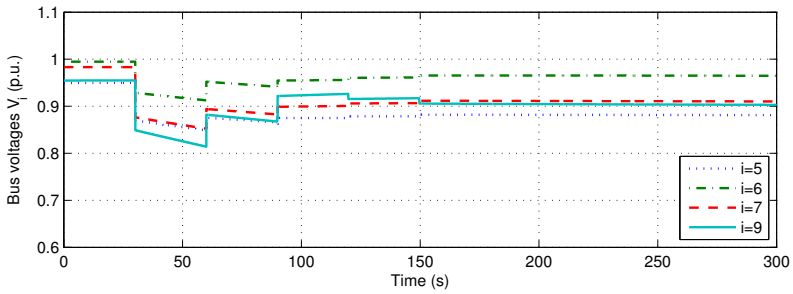

Figure 3.17: Bus voltage magnitudes (loss of generator g_2, nominal model).

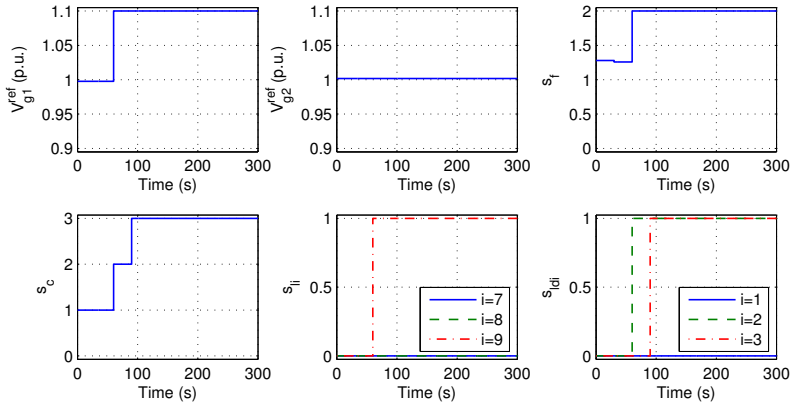

Figure 3.18: Control inputs (loss of generator g_2, nominal model).

works, the combination of discrete and continuous dynamics is found, and, hence, hybrid MPC problems have to be solved. The approach proposed here has the potential to do that.

Future research will focus on distributed predictive control, as the increase of the interconnections among countries leads to very large power networks with limited exchange of information. For industrial politics and security reasons, only partial knowledge of a subnetwork may be available to the others subnetworks, e.g., simplified subnetwork structures and dynamics. Control systems will have to deal efficiently with unpredictable disturbances, including unpredicted power flows and power outages in other subnetworks. Techniques from distributed optimization will be integrated in the approach proposed here to obtain an efficient distributed predictive control approach for hybrid systems.

Acknowledgements This research was partially carried out at Supélec–IETR, Hybrid Systems Control Group, Cesson-Sévigné, France. The authors would like to thank J. Buisson from Supélec-IETR, Rennes, France and J.L. Coullon from Areva Transport and Distribution, Massy, France for their support. This research is supported by the BSIK project "Next Generation Infrastructures (NGI)" and the Delft Research Center Next Generation Infrastructures.

References

1. E. Allen, N. LaWhite, Y. Yoon, J. Chapman, and M. Ilić. Interactive object-oriented simulation of interconnected power systems using Simulink. *IEEE Transactions on Education*, 44(1):87–95, February 2001.
2. P. J. Antsaklis. A brief introduction to the rheory and applications of hybrid systems. *IEEE Proceedings, Special Issue on Hybrid Systems: Theory and Applications*, 88(7):879–886, July 2000.
3. P. Barton and C. Pantelides. Modeling of combined discrete/continuous processes. *AIChE Journal*, 40(6):966–979, June 1994.
4. A. Bemporad and M. Morari. Control of systems integrating logic, dynamics, and constraints. *Automatica*, 35(3):407–427, March 1999.
5. J. Bernussou and A. Titli. *Interconnected Dynamical Systems: Stability, Decomposition and Decentralisation*. North-Holland Publishing Company, Amsterdam, The Netherlands, 1982.
6. L. T. Biegler, A. M. Cervantes, and A. Wachter. Advances in simultaneous strategies for dynamic process optimization. *Chemical Engineering Science*, 57(4):575–593, February 2002.
7. L. G. Bleris, P. D. Vouzis, J. G. Garcia, M. G. Arnold, and M. V. Kothare. Pathways for optimization-based drug delivery. *Control Engineering Practice*, 15(10):1280–1291, October 2007.
8. K. E. Brenan, S. L. Campbell, L. R., and Petzold. *Numerical Solution of Initial-Value Problems in Differential-Algebraic Equations*. SIAM, Philadelphia, Pennsylvania, 1996.
9. A. M. Cervantes and L. T. Biegler. Large-scale DAE optimization using a simultaneous NLP formulation. *AIChE Journal*, 44(5):1038–1050, May 1998.
10. I. K. Cho and H. Kim. Market power and network constraint in a deregulated electricity market. *The Energy Journal*, 28(2):1–34, April 2007.
11. M. Diehl, H. G. Bock, and J. P. Schlöder. A real-time iteration scheme for nonlinear optimization in optimal feedback control. *SIAM Journal on Control and Optimization*, 43(5):1714–1736, October 2005.
12. M. Diehl, H. G. Bock, J. P. Schlöder, R. Findeisen, Z. Nagy, and F. Allgöwer. Real-time optimization and nonlinear model predictive control of processes governed by differential-algebraic equations. *Journal of Process Control*, 12(4):577–585, June 2002.
13. Dynasim AB. *Dymola – Dynamic Modeling Laboratory, User's Manual*. Lund, Sweden, 2004.
14. Dynasim AB. Dymola-Simulink interface, 2004.
15. H. Elmqvist, S. E. Mattsson, and M. Otter. Modelica - a language for physical system modeling, visualization and interaction. In *Proceedings of the 1999 IEEE Symposium on Computer-Aided Control System Design*, pages 630–639, Kohala Coast, Hawaii, August 1999.
16. C. A. Falcone. Transmission in transition: bringing power to market. *IEEE Power Engineering Review*, 19(18):11–36, August 1999.
17. C. W. Gear. Differential-algebraic equation index transformation. *SIAM Journal on Scientific Computing*, 9(1):39–47, January 1988.
18. T. Geyer, M. Larsson, and M. Morari. Hybrid control of voltage collapse in power systems. In *Proceedings of the European Control Conference 2003*, volume 9, pages 157–166, Cambridge, UK, September 2003.
19. M. Ilić and J. Zaborsky. *Dynamics and Control of Large Electric Power Systems*. Wiley-Interscience, New York, New York, 2000.
20. N. Jenkins, R. Allan, P. Crossley, D. Kirschen, and G. Strbac. *Embedded Generation*. TJ International, Padstow, UK, 2000.
21. S. Kameswaran and L. T. Biegler. Simultaneous dynamic optimization strategies: Recent advances and challenges. *Computers and Chemical Engineering*, 30(10–12):1560–1575, September 2006.

22. D. Karlsson, M. Hemmingsson, and S. Lindahl. Wide area system monitoring and control - Terminology, phenomena, and solution implementation strategies. *IEEE Power and Energy Magazine*, 2(5):68–76, September–October 2004.
23. D. Karlsson and D.J. Hill. Modelling and identification of nonlinear dynamic loads in power systems. *IEEE Transactions on Power Systems*, 9(1):157–166, February 1994.
24. J. H. Kim, J. B. Park, J. K. Park, and S. K. Joo. A market-based analysis on the generation expansion planning strategies. In *Proceeding of the 13th International Conference on Intelligent Systems Application to Power Systems*, page 6, Washington, District of Columbia, November 2005.
25. P. Kundur. *Power System Stability and Control*. McGraw-Hill, New York, New York, 1994.
26. M. Larsson, D. J. Hill, and G. Olsson. Emergency voltage control using search and predictive control. *International Journal of Electric Power and Energy systems*, 24(2):121–130, February 2002.
27. R. Lazimy. Mixed-integer quadratic programming. *Mathematical Programming*, 22(1):332–349, December 1982.
28. S. Leirens. *Approche hybride pour la commade prédictive en tension d'un réseau d'énergie électrique*. PhD thesis, Supélec–Université de Rennes I, Rennes, France, December 2005.
29. S. Leirens and J. Buisson. An efficient algorithm for predictive control of piecewise affine systems with mixed inputs. In *Proceedings of the 2nd IFAC Conference on Analysis and Design of Hybrid Systems*, pages 309–314, Alghero, Italy, June 2006.
30. J. T. Linderoth and T. K. Ralphs. Noncommercial software for mixed-integer linear programming. Technical Report 04T-023, Department of Industrial and Systems Engineering, Lehigh University, Bethlehem, Pennsylvania, December 2004.
31. J. M. Maciejowski. *Predictive Control with Constraints*. Prentice-Hall, Harlow, UK, 2002.
32. Y. Majanne. Model predictive pressure control of steam networks. *Control Engineering Practice*, 13(12):1499–1505, December 2005.
33. A. Manzonic, A. S. de Silva, and I. C. Decker. Power systems, dynamics simulation using object-oriented programming. *IEEE Transactions on Power Systems*, 14(1):249–255, February 1999.
34. The MathWorks. MATLAB and Simulink for Technical Computing, 2009.
35. S. E. Mattsson, H. Elmqvist, and M. Otter. Physical system modeling with Modelica. *Control Engineering Practice*, 6(4):501–510, April 1998.
36. D. Q. Mayne, J. B. Rawlings, C. V. Rao, and P. O. M. Scocaert. Constrained model predictive control: Stability and optimality. *Automatica*, 36(6):789–814, June 2000.
37. D. Mignone. *Control and Estimation of Hybrid Systems with Mathematical Optimization*. PhD thesis, Swiss Federal Institute of Technology (ETH), Zürich, Switzerland, 2002.
38. Modelica Association. *Modelica - A Unified Object-Oriented Language for Physical Systems Modeling, Language Specification Version 3.0*, September 2007.
39. A. Monticelli. Electric power system state estimation. *Proceedings of the IEEE*, 88(2):262–282, February 2000.
40. M. Morari and J. H. Lee. Model predictive control: Past, present and future. *Computers and Chemical Engineering*, 23(4):667–682, 1999.
41. I. R. Navarro, M. Larsson, and G. Olsson. Object-oriented modeling and simulation of power systems using Modelica. In *Proceedings of the IEEE Power Engineering Society Winter Meeting*, pages 790–795, Singapore, January 2000.
42. R. R. Negenborn, M. Houwing, B. De Schutter, and J. Hellendoorn. Model predictive control for residential energy resources using a mixed-logical dynamic model. In *Proceedings of the 2009 IEEE International Conference on Networking, Sensing and Control*, pages 702–707, Okayama, Japan, March 2009.
43. R. R. Negenborn, S. Leirens, B. De Schutter, and J. Hellendoorn. Supervisory nonlinear MPC for emergency voltage control using pattern search. *Control Engineering Practice*, 17(7):841–848, July 2009.

44. R. R. Negenborn, P. J. van Overloop, T. Keviczky, and B. De Schutter. Distributed model predictive control for irrigation canals. *Networks and Heterogeneous Media*, 4(2):359–380, June 2009.
45. L. R. Petzold. A differential/algebraic system solver. In *Proceedings of the 10th World Congress on System Simulation and Scientific Computation*, pages 430–432, Montreal, Canada, August 1983.
46. P. C. Piela, T. G. Epperly, K. M. Westerberg, and A. W. Westerberg. ASCEND: an object-oriented computer environment for modeling and analysis: The modeling language. *Computers and Chemical Engineering*, 15(1):53–72, January 1991.
47. S. Piñón, E. F. Camacho, B. Kuchen, and M. Peña. Constrained predictive control of a greenhouse. *Computers and Electronics in Agriculture*, 49(3):317–329, December 2005.
48. D. H. Popović, D. J. Hill, and Q. Wu. Coordinated static and dynamic voltage control in large power systems. In *Proceedings of the Bulk Power System Dynamics and Control IV – Restructuring*, Santorini, Greece, August 1998.
49. Power System Stability Subcommittee. Voltage stability of power systems: Concepts, analytical tools and industry experience. Technical Report 90TH0358-2-PWR, IEEE/PES, 1990.
50. Power System Stability Subcommittee. Voltage stability assessment: Concepts, practices and tools. Technical Report SP101PSS, IEEE/PES, August 2002.
51. C. Rehtanz, M. Larsson, M. Zima, M. Kaba, and J. Bertsch. System for wide area protection, control and optimization based on phasor measurements. In *Proceedings of the International Conference on Power Systems and Communication Systems Infrastructures for the Future*, Beijing, China, September 2002.
52. C. A. Ruiz, N. J. Orrego, and J. F. Gutierrez. The Colombian 2007 blackout. In *Proceedings of the IEEE/PES Transmission and Distribution Conference and Exposition: Latin America*, pages 1–5, Bogotá, Colombia, aug 2008.
53. UCTE. Interim report of the investigation committee on the 28 September 2003 blackout in italy. Technical report, UCTE, 2004.
54. U.S.–Canada Power System Outage Task Force. Final report on the August 14, 2003 blackout in the USA and Canada: causes and recommendations. Technical report, U.S. Department of Energy, Natural Resources Canada, 2004.
55. T. Van Cutsem and C. Vournas. *Voltage Stability of Electric Power Systems*. Kluwer Academic Publishers, Dordrecht, The Netherlands, 1998.
56. Wolfram Research. Mathematica, Technical and Scientific Software, 2007.